Simulation Studies of a Helical *m*-Phenylene Ethynylene Foldamer

One-Sun Lee and Jeffery G. Saven*

Makineni Theoretical Laboratories, Department of Chemistry, 231 South 34th Street, University of Pennsylvania, Philadelphia, Pennsylvania 19104

Received: March 27, 2004; In Final Form: June 3, 2004

The folded state of an oligo(*m*-phenylene ethynylene) foldamer solvated in water is examined using a 30 ns NpT molecular dynamics simulation. The 18-monomer oligomer with methyl ester exterior side groups maintains a helical structure, where turns of the helix are in close contact throughout the simulation. The structure exhibits large fluctuations in both the radius of the interior cylindrical pore and the effective dihedral angle between monomers. The radius fluctuations are correlated with the number of water molecules within the helical pore. The folded state is found to be surprisingly flexible while maintaining a helical structure.

Introduction

Helical structures are common folding motifs among the biopolymers: proteins, DNA, and RNA. More recently, helical secondary structures have also been realized using synthetic, nonbiological oligomers.[1,2] As with the biopolymers, the folded conformations of such nonbiological foldamers are determined by the allowed conformational states of the backbone and are stabilized by noncovalent interactions such as hydrogen bonding, hydrophobic interactions, and van der Waals forces.[2] The design and synthesis of nonbiological molecules that adopt helical conformations in solution has been an active area of research.[2,3] In addition to informing our understanding of molecular folding, the study of helical nanoscale foldamers may provide novel structures for molecular recognition, catalysis, and biomaterials in the form of drug delivery materials and electronics.[2−5] Many of these molecules have helical cores that are tightly packed, as is the case with the α-helix of α amino acids. With alternate backbones, however, the radius of the helix may be large enough to present an interior tubular cavity. Such a helical cavity provides an inherently chiral, asymmetric environment that has been used for enantioselective host−guest recognition.[6,7] Herein, the use of molecular dynamics simulation is used to probe the flexibility and structural fluctuations of one class of helical foldamers.

Recently, Moore and co-workers have reported a series of novel synthetic oligo(*m*-phenylene ethynylene) oligomers that reversibly fold into well-defined helical structures.[8] The oligomers comprise *meta*-substituted phenylene ethynylene monomers (Figure 1). Many monomer types are available, and a variety of exterior side chains may be introduced so as to modulate solubility and stability. Chiral monomers and side groups may also be substituted into the chain so as to bias one handedness of the folded helical structure.[9,10] The helical folded states of phenylene ethynylene oligomers are stabilized by van der Waals forces, electrostatic interactions, and solvophobic effects.[11] The oligomers exhibit the properties of an unstructured random coil in "good" solvents such as chloroform, whereas they fold into a helical structure in "poor" solvents such as acetonitrile.[8,12] Surprisingly, the helical folded structure is robust and persists in a wide variety of polar and nonpolar organic solvents.[13] The folded structure possesses an ordered pore, which has been functionalized so as to capture selectively a variety of metals with appropriately patterned functional groups.[14] In addition, the helical structure provides an asymmetric, enantiomeric binding surface. Chiral molecules can be bound inside the oligomer pore, and the free energy differences between diastereomeric complexes are sufficient to obtain molecular recognition.[7,15,16]

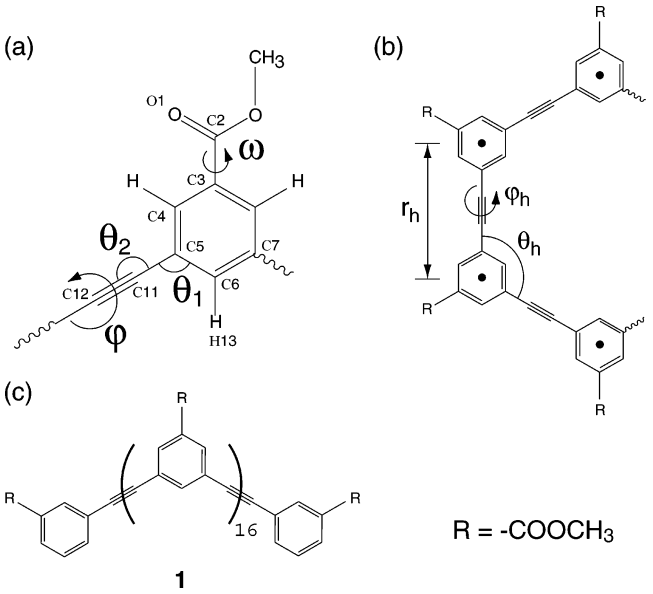

1

Figure 1. (a) Structure of *m*-phenylene ethynylene monomer. The dihedral angle, φ, is defined with C6−C5−C7′−C6′ atoms on adjacent monomers, and ω is defined with C4−C3−C2−O1 atoms. The angles θ_1 and θ_2 are defined with C6−C5−C11 and C5−C11−C12 atoms, respectively. (b) Structural parameters of r_h, θ_h, and φ_h, each defined using the centers of mass of the phenyl rings of adjacent monomers: r_h is the distance between monomers, θ_h is the effective bond angle involving three contiguous monomers, and φ_h is the effective dihedral angle inolving four contiguous monomers. (c) Schematic structure of 18-mer oligo(*m*-phenylene ethynylene) **1**. R is the CO_2CH_3 group in this study.

Much is known about the folded states of phenylene ethynylene oligomers from a variety of spectroscopic experiments,[8,11,12] and high-pressure studies have found that the helical,

* Corresponding author. Telephone: (215) 573-6062. Fax: (215) 573-0980. E-mail: saven@sas.upenn.edu.

10.1021/jp048642m CCC: $27.50
Published on Web 07/16/2004

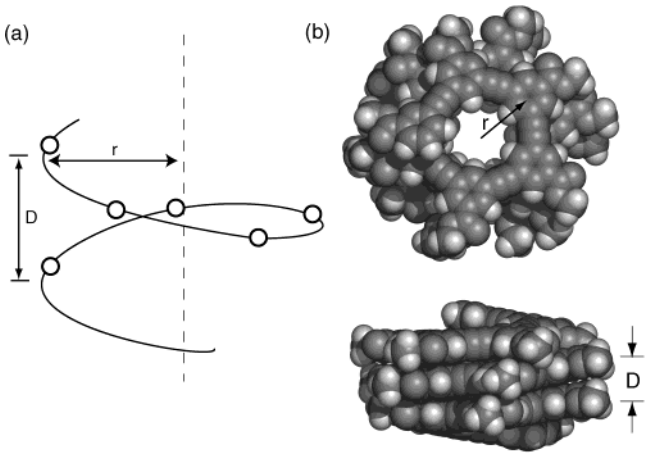

Figure 2. (a) The schematic helical structure of **1**. Centers of the phenyl rings in the monomers are represented by circles. (b) Top and side views of the energy-minimized structure. (All space filling images were rendered using PyMOL.[53]) The radius *r* is defined as the distance between the axis of the helix that best fits a given conformation. The helix is fit to the centers of mass of the phenyl rings of the monomers. For such a fitted helix, the pitch *D* is defined as the distance between turns.

folded state exhibits increased compressibility.[6] Presently, we have no experimentally determined information, however, concerning the helical structure and its dynamics at atomic resolution. Molecular simulations may be used to probe such structural fluctuations. There have been several simulation-based investigations involving the folding and dynamic properties of oligo(*m*-phenylene ethynylene)s. Elmer and Pande used an implicit solvent model and Langevin dynamics to simulate the folding of an oligo(*m*-phenylene ethynylene).[17] In agreement with experiment, the folding time was estimated to be 50 ns and the observed nonexponential kinetics exhibited on-pathway intermediate states.[18] In studying the structural properties of the folded state, however, it would be preferable to use explicit solvent models. Sen has studied the dynamic properties of oligo(*m*-phenylene ethynylene) using molecular dynamics simulation.[19] He found that the helical structure of the oligomer is not only stabilized by solvophobic interactions but also by favorable contributions from the van der Waals interactions. Sen also studied the behavior of water molecules inside the pore of the helical structure. He found that the residence time of water molecules inside the oligomer is 10−100 ps, and their behavior is very different from that of the bulk water. However, Sen used a largely unmodified form of the CHARMM potential, which has been parametrized for proteins, and considered a relatively short total simulation time, 0.75 ns. Longer molecular dynamics simulations with more refined potential parameters appropriate for the oligo(*m*-phenylene ethynylene) oligomers are needed for a detailed understanding of the structural fluctuations available to these oligomers in a solvated environment.

Here, we report the structural fluctuations and dynamics of an oligo(*m*-phenylene ethynylene) 18-mer, **1** (see Figure 1c). A system comprising the oligomer **1** is solvated in water and simulated for 30 ns using molecular dynamics simulation with the isothermal−isobaric (NpT) ensemble. New force-field parameters for the oligomer were developed using experimental and quantum mechanical results. Structural features and fluctuations of **1** are represented by structural and helical parameters at a molecular level (see Figures 1 and 2). A global minimum energy helical structure is obtained by energy minimization, and this structure provides a useful reference with which to compare transiently generated structures during the course of the molecular dynamics simulation. The interaction between **1** and water molecules is also monitored, and the residence times of water molecules inside **1** are measured. During the simulation, **1** maintains a helical structure, which tolerates large fluctuations in the diameter of the cavity and in the effective dihedral angles between monomers. The average number of water molecules inside the helix is 4.6 ± 3.8, and the mean residence time of the water molecules is 7.1 ps.

TABLE 1: Force-Field Parameters for *m*-Phenylene Ethynylene Monomer (See Figure 1 and Eqs 1 and 2)

angle	k_θ (kcal/mol/rad^2)	θ_0 (deg)	
θ_1	75.0	120.0	
θ_2	44.5	180.0	
dihedral	**k_χ (kcal/mol)**	**n**	**d**
ϕ	0.12	2	180
ω	3.95	2	180

Methods

New force-field parameters for **1** were developed consistent with experimental results or quantum mechanical calculations. For the methyl ester monomers depicted in Figure 1, the restrained electrostatic potential method[20,21] was used to obtain effective atomic charges subject to overall neutrality of each monomer. The effective charges were fit using electrostatic energies computed using the HF/6-311G** basis set in Gaussian 98.[22] For the dihedral angle φ between the benzene rings of two adjacent monomers (see Figure 1), the dihedral potential was fit to the barrier height (0.6 kcal/mol) suggested by the experimental results by Okuyama et al.,[23] which is within 10% of that predicted by quantum chemical calculations.[24] The parameters for the potential energies involving θ_1, θ_2, and ω were developed by varying structure and fitting the relative energies obtained from quantum mechanical calculations (with the HF/6-311G** basis set) using standard functional forms. The equation for the bond angle term is

$$E(\theta) = k_\theta(\theta - \theta_0)^2 \quad (1)$$

and the equation for the dihedral term is

$$E(\chi) = k_\chi(1 + \cos(n\chi - \delta)) \quad (2)$$

The parameters fitted to the experimental or quantum mechanical results are listed in Table 1. (The calculated partial charges on the monomer are contained in the Supporting Information.) Other force-field parameters not discussed here are obtained from the CHARMM22 force field.[25]

Macromodel 7.0[26] was used to build the initial structure of the right-handed (*P*) helix of oligomer **1**. An energy-minimized helical structure was solvated in a water box using the SOLVATE module[27] implemented in VMD.[28] Periodic boundary conditions were used corresponding to a box of dimensions 60 × 60 × 60 Å^3. This box was filled with 6633 molecules of modified TIP3P water,[25,29] and only one water molecule was placed inside the cavity of **1** in the initial configuration. An additional 10 steps of energy minimization was applied to the solvated system to remove the high-energy contacts. No atomic coordinates were constrained during subsequent molecular dynamics calculations.

Molecular simulations were carried out using NAMD2[30] with the CHARMM22 force field.[31] Annealing molecular dynamics was applied to this oligomer−water system with NpT ensemble. The temperature, initially set at 400 K, is lowered by 25 K after every 100 ps, until it has reached 300 K. The system was then

evolved at 300 K for an additional 100 ps. This annealed structure is used as a starting configuration for the next production molecular dynamics simulation. In the production period, the system was simulated for 30 ns in the NpT ensemble using Langevin dynamics at a temperature of 300 K with a damping coefficient of $\gamma = 5\ \mathrm{ps}^{-1}$. Pressure was maintained at 1 atm using the Langevin piston method with a piston period of 100 fs, a damping time constant of 50 fs, and piston temperature of 300 K.[32,33] Full electrostatics was employed using the particle-mesh Ewald[34] method with 1 Å grid width. Nonbonded interactions were calculated using a group-based cutoff with a switching function and were updated every 5 time steps. A time step of 1 fs was used, and atomic coordinates were saved every 1 ps for the trajectory analysis. For comparison with previous studies,[8] molecular minimization of **1** in a vacuum is also performed to obtain low-energy structures.

For the analysis of the molecular structures, helix parameters for **1** were calculated for every saved structure from the molecular dynamics calculation. Helical parameters were obtained by fitting a regular helix to the centers of mass of each monomer's aromatic ring.[35] The equation of a general helix, after translation by the vector displacement $\boldsymbol{p}$ and application of a suitable rotation matrix $\boldsymbol{R}$, can be written as

$$\boldsymbol{\gamma}(t) = \begin{bmatrix} r\cos(\omega t) \\ r\sin(\omega t) \\ t\nu_z \end{bmatrix} \tag{3}$$

where ω is the angular frequency and ν_z is the rise along the helical axis per monomer. Thus, the problem is to find the set of parameters of the helix [r, ω, ν_z, $\boldsymbol{p}$, $\boldsymbol{R}$] that minimize the summation of the distance between the helix and the given points. The objective function can be written as

$$F = \sum_{t=1}^{N} |\boldsymbol{R}\cdot\boldsymbol{\gamma}(t) + \boldsymbol{p} - \boldsymbol{q}_t|^2 \tag{4}$$

where $\boldsymbol{q}_t$ is the position of the tth monomer. F is minimized to obtain the helix parameters. The number of monomers per turn of helix is $n \equiv 2\pi/\omega$, and the pitch of the helix, $D \equiv n\nu_z$, may be calculated from the fit for a given structure of the oligomer.

Results and Discussion

In this study, appropriate potential parameters and partial charges have been determined for the monomer shown in Figure 1. For the two-fold symmetric potential involving φ, the experimentally estimated rotational barrier (where adjacent phenyl rings are perpendicular) in tolane is 0.6 kcal/mol,[23] and this is the value used herein. Similarly, this barrier height has also been estimated to be 0.64 kcal/mol, using quantum mechanical calculations with the MP2/6-311G** basis set.[24] With the potential parameters reported in a previous study, however, the barrier height for φ was approximately 5 kcal/mol.[19] The average value of the angle ω is expected to be 0° or 180° so as to maintain coplanarity of the carboxylate OCO group and the phenyl ring (see Figure 1). Herein, the estimated rotational barrier for ω is 7.9 kcal/mol, according to a quantum mechanical calculation with the HF/6-311G** basis set. This value is consistent with theoretical estimates of the corresponding barrier height in benzoic acid and ethyl benzoate: 5−9 kcal/mol.[36,37] On the other hand, a previous simulation of an oligo(phenylene ethynylene) reported average values of $\omega = 81°$ and $\omega = -76°$.[19] For θ_2, quantum mechanical calculations suggest that this angle is not perfectly rigid and thermal fluctuations on the order of ±7° are accessible,[38] which is consistent with the low calculated frequency for this bend (see Table 1). Even though this range of bending of θ_2 is small, it can greatly influence the fluctuations of the radius of the helical structure of the oligomer, because there are 10−12 θ_2 angles in one turn, where the number of monomers per turn is n = 5−6.

The potential energy-minimized structure of **1** in vacuo is presented in Figure 2b. In this fitted helix structure, the radius is 6.3 Å and the number of monomers per turn is 5.7. Thus, the contacting monomers between turns must be slightly staggered. The pitch D is 3.8 Å, which is consistent with the turns of the helix being near van der Waals contact. The value of the pitch is comparable to the stacking of aromatic rings as observed in quantum mechanical and force-field investigations of benzene and toluene dimers,[39] where the equilibrium center−center distance of the stacked dimer is 3.8 Å. In the minimized helical structure of **1**, the energy contributions of the van der Waals and electrostatic terms are 21% and 63%, respectively. Although the potential does not explicitly address the polarizability of the aromatic groups, this decomposition of intermonomer interactions is consistent with the dominant types of intermolecular forces associated with aromatic interactions:[39] van der Waals forces and electrostatic terms.[40] While van der Waals interactions play a large role in the attractive forces between aromatic groups, these interactions are degenerate, and the turns of the helix may slide while maintaining interturn contacts. Electrostatic interactions likely specify orientation among interacting aromatic groups.[40,41] For the force field employed herein, low-energy orientations are determined largely by the partial charges on the atoms. Recently, the importance of the carboxyl side-chain dipole moment on the orientation of phenyl ethynylene foldamers has been discussed.[42] The methyl ester side groups separated by one turn of the helix may be in either syn or anti configurations, and the configuration may be difficult to control experimentally due to the large barrier for ω. For the *m*-phenylene ethynylene oligomer **1** simulated herein, an all-syn configuration was chosen, and in the low-energy structure, the side chains of monomers in adjacent turns are staggered. Because the partial charges on remaining atoms are independent of ω, the observed dynamical features are expected to be robust with regard to alternate configurations of the ester groups. Nonetheless, it may be of interest to study such alternate syn/anti configurations in future work.

The energy-minimized helical molecule provides a useful reference for trajectory analysis of molecular dynamics. Equation 5 is used for calculating the RMSD after translation and minimization of a given structure onto the reference structure,[43] where x_i and $x_i^{\min}$ are the coordinates of the ith backbone atom of a structure and the minimum energy structure in a vacuum.

$$\mathrm{RMSD}(x,x^{\min}) = \left[\frac{1}{M}\sum_{i=1}^{M}\left|x_i - x_i^{\min}\right|^2\right]^{1/2} \tag{5}$$

The backbone comprises those M atoms that are in the phenylene ethynylene main chain of the oligomer; atoms in the side chains R are excluded. Averaged over the entire 30 ns trajectory, the RMSD is 2.1 ± 1.2 Å. (All statistical uncertainties are $\pm 2\sigma$ (two standard deviations).) Interestingly, the oligomer retains its helical structure throughout the calculation and never unfolds or samples the other enantiomer of the helical folded state.

During the 30 ns molecular dynamics simulation, the distributions of the structural parameters, r_h, θ_h, and φ_h (see Figure 1), are monitored, and the numbers of distinct values

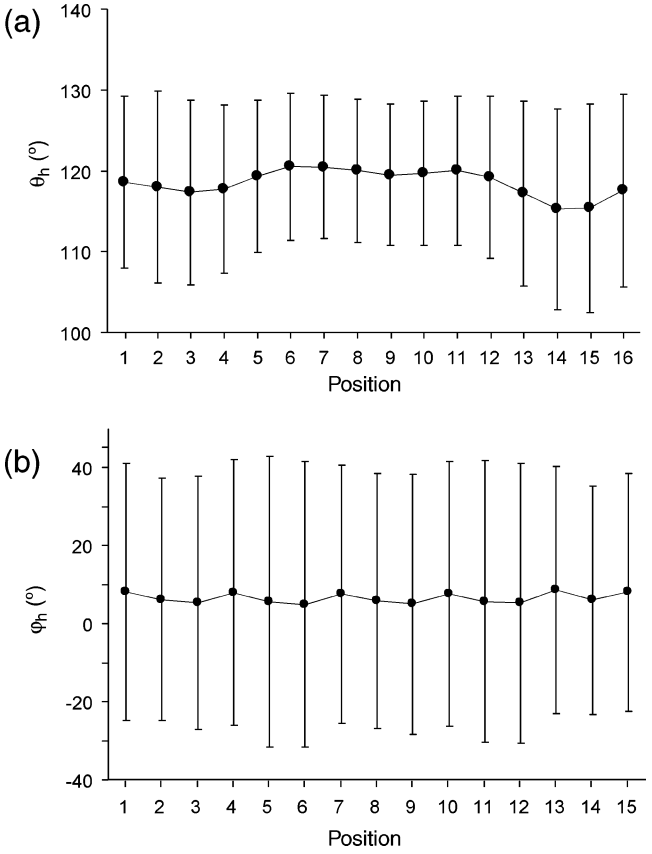

Figure 3. Monomer-dependent values of θ_h (a) and φ_h (b). The mean value of θ_h is 120.0° ± 9.0° for middle positions, whereas it is 117.6° ± 11.6° for the two ends. The mean value of φ_h over all positions is 6.6° ± 33.6°.

for these parameters are 17 ($N - 1$), 16 ($N - 2$), and 15 ($N - 3$), respectively. The mean and standard deviation for each quantity are calculated for the 30 ns MD trajectory. The distance between two monomers r_h is almost constant $r_h = 6.8 \pm 0.1$ Å, consistent with the relatively incompressible ethynylene linkage between neighboring monomeric rings. In Figure 3a, the distribution of the angle θ_h is presented. This angle is defined using the centers of mass of three contiguous monomers. The value of θ_h is slightly smaller at the two end positions than in the middle, indicating a tighter coiling of the helix for the terminal regions. θ_h is nearly 120° for interior positions, whereas $\theta_h = 117°$ for the two ends. The large error bars on θ_h suggest that the helical structure accommodates marked fluctuations (110−128°) in this angle and is slightly less rigid at the ends than in the interior positions.

The distribution of the effective dihedral angle φ_h is shown in Figure 3b, where φ_h is defined using the centers of mass of the phenyl rings of four contiguous monomers. The mean value of φ_h for each position is $\varphi_h = 6.6° \pm 33.6°$. Unlike the θ_h distribution, the relative fluctuations in φ_h are large. We might expect such large fluctuations given the intrinsically low barrier to free rotation about this dihedral angle, 0.6 kcal/mol, which is on the order of k_BT. Surprisingly, these large fluctuations maintain the helical structure. The average value of the angle in each case is positive, as it must be if the oligomer is to form a right-handed *P* helix. Nonetheless, φ_h takes on negative values, which would seem incompatible with the chosen handedness of the helix. The values of adjacent φ_h are highly correlated, however, and if one of the φ_h has a negative value, on average, the adjacent φ_h has a large positive value so as to compensate and maintain the helical structure (see Figure 4). The helix is tolerant of these dihedral fluctuations because contacting monomers in neighboring turns may slide with respect to one another without disrupting the global helical structure. The large aromatic surfaces tolerate shifts in orientation while maintaining their van der Waals interactions.[44] In contrast, the dihedral angles are far more constrained for helices that are specified by highly

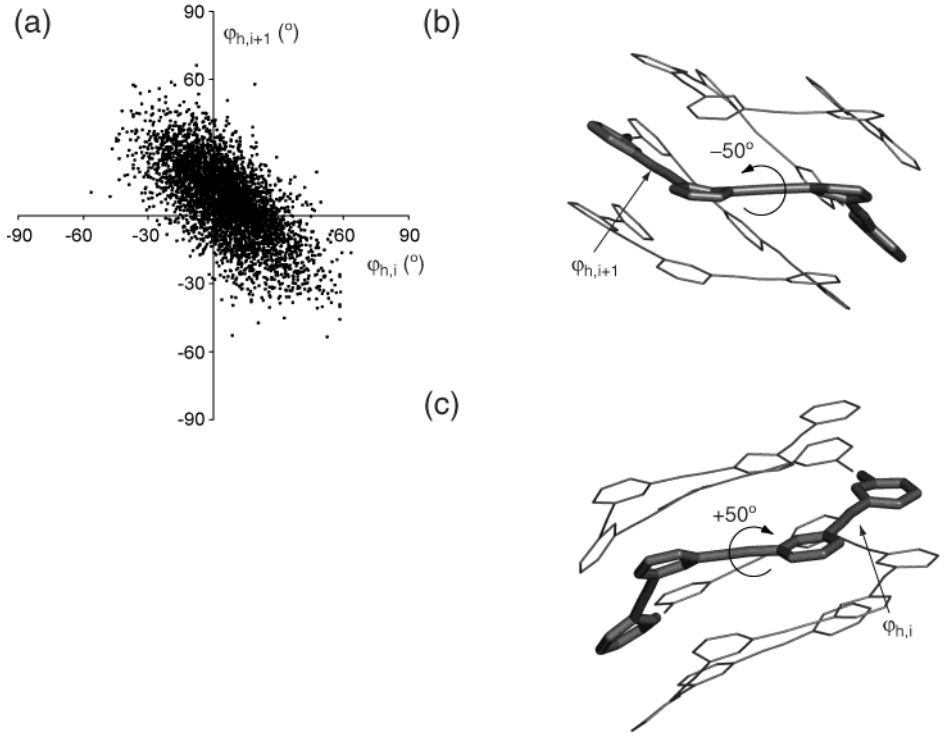

Figure 4. (a) Scatter plot of $\varphi_{h,i}$ and $\varphi_{h,i+1}$. Extreme values of each are anti-correlated: if one of the φ_h has a small or negative value, an adjacent $\varphi_{h,i+1}$ has a large positive value so as to compensate and keep the whole structure helical. (b and c) Two adjacent φ_h angles, illustrating the change in sign for large values of φ_h. Side chains and hydrogen atoms are omitted for clarity.

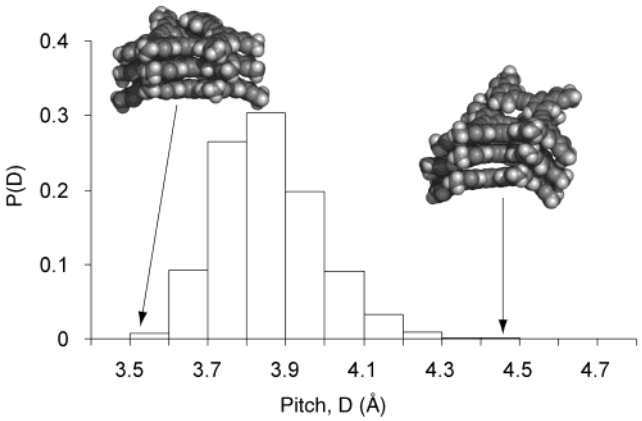

Figure 5. The distribution of pitch *D*. The rendered structures are representative of the indicated values of *D*.

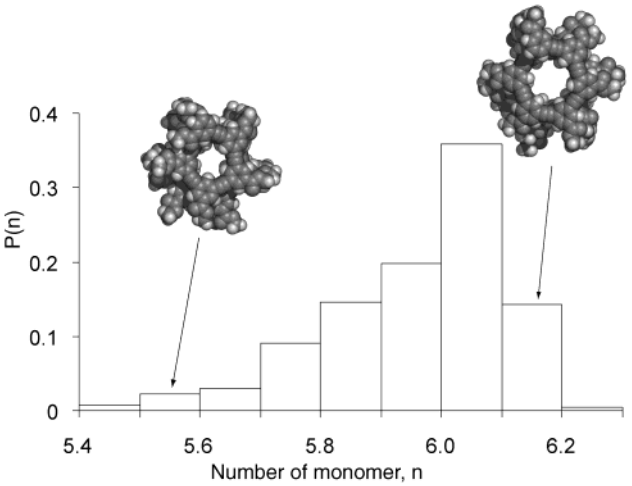

Figure 6. The distribution of number of monomer per one turn *n*. The rendered structures are representative of the indicated values of *n*.

specific and directional interactions such as hydrogen bonds, for example, the α helix of peptides, as is evidenced by a well-defined helical region in the Ramachandran map.

The mean value of the pitch is $D = 3.9 \pm 0.2$ Å (Figure 5), and the pitch takes on values in the range $D = 3.6-4.2$ Å, suggesting a slight vertical flexibility associated with the helix. Nonetheless, the individual turns of the helix nearly maintain van der Waals contact despite the large fluctuations in other structural quantities.

The fluctuations in the number of monomers per turn and especially the radius of the helical structure are much more pronounced. The distribution of *n* is in Figure 6. While the average number of monomers per helical turn is $n = 6.0 \pm 0.2$, the distribution suggests that fluctuations having 5.5−6.2 monomers per turn are common. The monomers are nearly cofacially stacked at the most probable value near $n = 6.0$. The mean value of *r* for whole simulation is $r = 6.5 \pm 0.4$ Å. The distribution of *r* is in Figure 7. Fluctuations in the helical radius over the range 5.7−6.7 Å are observed, which is consistent with fluctuations of approximately 2 Å in the interior diameter of the helix.

There have been many simulations of nanotubes and nanopores in water to monitor the behavior of water molecules inside the tube.[19,45−47] In many simulations, the filling and emptying of water molecules inside hydrophobic pores has been observed. One study, however, reported that water molecules inside an oligomer similar to **1** form a hydrogen-bonding network, and some molecules reside within the helix for approximately 100

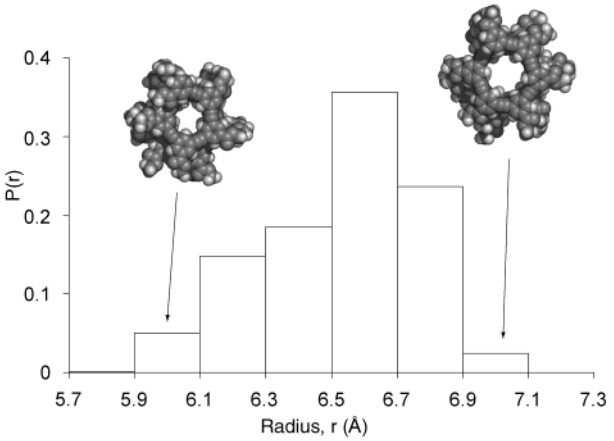

Figure 7. The distribution of radius *r*. The rendered structures are representative of the indicated values of *r*.

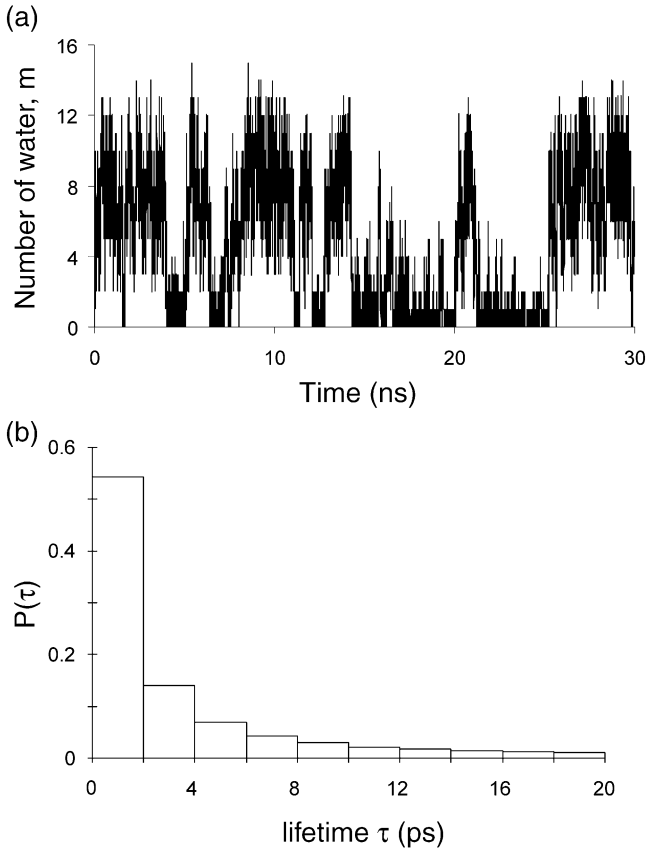

Figure 8. (a) The fluctuation of number of water molecules *m* inside **1** during the 30 ns MD simulation. The mean value is $m = 4.6 \pm 3.8$. (b) The distribution of residence times of water inside **1**. The mean residence time is 7.6 ps, and 83% of the distribution is less than 10 ps.

ps.[19] The water molecules inside carbon nanotubes form a one-dimensional wire-like hydrogen-bonding arrangement,[45] while the water molecules form a H-bonded cluster in the *m*-phenylene ethynylene oligomer because the helix pore is larger.[19]

It is of interest then to monitor solvent molecules within the interior cavity. In calculating the number of interior water molecules, the eight H13-type hydrogen atoms in middle position of the helix (positions 6−13) were used; a water molecule resides in the helix cavity if it is within 4 Å of any of these six interior hydrogen atoms. The fluctuation in the number of water molecules *m* inside **1** is shown in Figure 8a. The average number of waters is $m = 4.6 \pm 3.8$, and the highest number is $m = 15$. The lifetimes of the filled states vary from

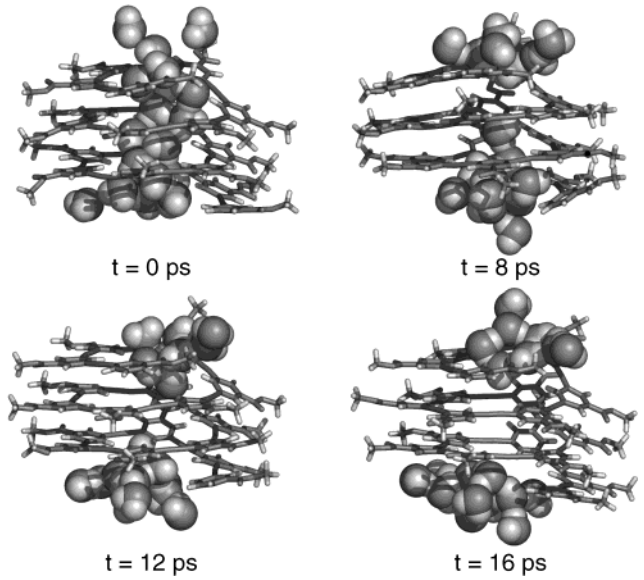

Figure 9. Snapshots of the emptying procedure of water from **1**. When hydrogen bonding is broken ($t = 8$ ps), water molecules recede to both ends of **1** ($t = 12$ and 16 ps).

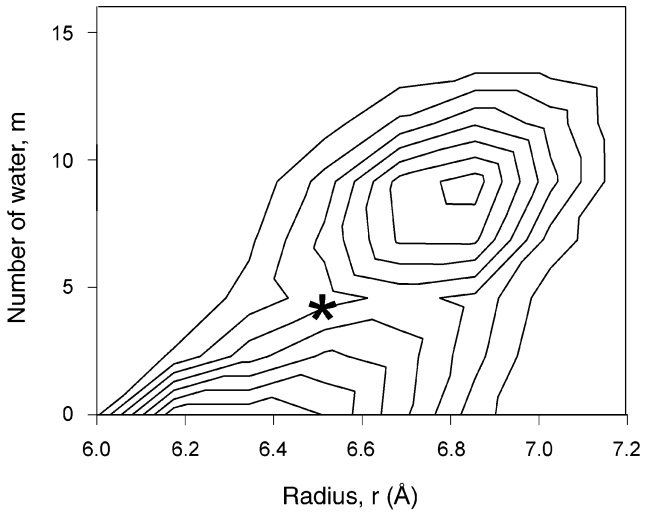

Figure 10. The contour map of the joint probability (normalized histogram) $P(r,m)$ as a function of the helical radius r and the number of water molecules inside the pore m. The spacing between contours is 1%; the lowest lying contour corresponds to $P(r,m) = 1\%$. The point represented by "*" indicates the mean values of $r = 6.5$ and $m = 4.6$.

tens of picoseconds to several nanoseconds. However, the time for changing state from filled to empty (or empty to filled) is relatively rapid, on the order of tens of picoseconds. The longest emptied state occurs from 15 to 20 ns and coincides with the decrease of radius. During this period, there is no significant change of pitch. The emptying is correlated with the decrease of radius, as was found in a previous simulation of a nanopore.[47] The filling and emptying procedures are found in many simulations of water-permeable pores.[45−48] In the work by Beckstein et al., water molecules were not observed to enter a pore if the radius was less than 4.5 Å, even though this radius was apparently large enough to accommodate three water molecules.[47] The pore radius is also observed to be an important factor for filling and emptying of water in the present simulation.

The distribution of residence times of water molecules inside the helical pore of **1** was also determined (see Figure 8b). About 83% of the residence times are less than 10 ps and the mean residence time is 7.1 ps. This lifetime is somewhat longer than that of a hydrogen bond between water molecules in bulk water (few picoseconds). Even though the mean residence time is relatively short, the distribution has a long tail, and the longest residence time observed is 186 ps. However, residence times longer than 100 ps involve less than 0.3% of the water molecules considered. Water inside **1** appears to form a hydrogen-bonded network rather than wire-like hydrogen bonding.

In filling the pore, water molecules can enter from both ends of helical **1**. When a water molecule approaches from one of the ends, it maintains hydrogen bonding with bulk water. If the inner space of the cavity is vacant, water molecules approach from both ends, and they meet and establish hydrogen bonding. The emptying of **1** seems to reverse this procedure of filling. The snapshots of the emptying process are in Figure 9. If hydrogen bonding breaks at the middle the interior cavity, water molecules rapidly recede (tens of picoseconds) to both ends of **1**.

The radius r fluctuations are correlated with m, the number of water molecules inside **1**, with r decreasing with decreasing m. The distribution of r and m is shown in Figure 10. There are two high population regions at $r = 6.8$ and $m = 8$ and at $r = 6.2$ and $m = 0$. The mean radius and the mean number of water molecules ($r = 6.5$, $m = 4.6$) is also shown and is intermediate between the two more populated regions. The results in Figures 8a and 10 suggest an apparent two-state behavior, where the foldamer fluctuates between an essentially empty state and one having 8−10 water molecules within the interior. The folded helical structure is able to tolerate large fluctuations in the interior radius so as to accommodate a range of molecular volumes. Herein, solvent is the interior "guest" molecule, and the large spontaneous fluctuations suggest that helical phenylene ethynylene oligomers are a versatile and flexible host motif for engineering a wide variety of host−guest systems.

Conclusion

During a 30 ns NpT molecular dynamics simulation of the *m*-phenylene ethynylene oligomer **1**, the molecule maintains its helical structure while simultaneously exhibiting large fluctuations in its structural features. The molecule is essentially rigid with respect to the average distances between adjacent monomers both along the backbone contour and between turns of the helix, as suggested by the small fluctuations in r_h and the pitch D. Surprisingly, the effective dihedral angle φ_h takes on a large range of values (see Figure 4), suggesting that a wide range of local orientations of monomers within the helical interior are explored. Correlated with the large fluctuations in the number of monomers per turn and the effective angle between monomers θ_h are the large fluctuations observed in the effective helical radius: the diameter of the pore may vary by more than 2 Å (12−14.4 Å), which is consistent with the ability of the foldamer to accommodate a wide variety of guest molecules and interior substituents.[1,7,49] While no such guest molecules were considered in these simulations, the behavior of solvent (water) within the interior pore was examined, and it was found that the pore can accommodate solvent molecules with numbers in the range 0−15. This is in qualitative agreement with high-pressure studies indicating the increased compressibility of the helical folded state.[6] We note that oligomer **1** is not likely to be water soluble, and simplified side chains have been used in the present simulation. Nonetheless, water-soluble variants of oligo(*m*-phenylene ethynylene)s have already been identified via the appropriate choice of the exterior side chains R.[49] It will be of interest to simulate and explore the dynamical features of these other variants of **1**, such as those with poly-

(ethylene glycol) side chains as opposed to the methyl esters considered herein. In addition, it will be of interest to compare the dynamical behavior of the molecule considered here with other related foldamers, such as oligo(*o*-phenylene ethynylene)s,[42,50] which have a smaller pore diameter and likely a more rigid helical structure.

The oligo(*m*-phenylene ethynylene)s such as oligomer **1** provide a highly flexible, chiral environment to bind a variety of guest molecules. A wide range of pore sizes was observed in the simulation, suggesting the scaffold can accommodate guest molecules with a wide range of molecular sizes and dimensions. Combined with the many monomer types that are available with these foldamers, the pliability of the helical structure observed in these simulations suggests that *m*-phenylene ethynylene oligomers are a promising scaffold for the elaboration of tight binding host−guest systems and catalysts, where conformational flexibility may be required for turnover.[51,52]

Acknowledgment. We acknowledge support from the National Science Foundation (CHE 9984752 and CHE 0345254). J.G.S. is a Cottrell Scholar of Research Corporation and an Arnold and Mabel Beckman Foundation Young Investigator. NAMD was developed by the Theoretical and Computational Biophysics Group in the Beckman Institute for Advanced Science and Technology at the University of Illinois at Urbana-Champaign. We thank T. Karatas for sharing his helix fitting algorithms.

Supporting Information Available: Atomic charges used in the simulation. This material is available free of charge via the Internet at http://pubs.acs.org.

References and Notes

(1) Hill, D. J.; Mio, M. J.; Prince, R. B.; Hughes, T. S.; Moore, J. S. *Chem. Rev.* **2001**, *101*, 3893.
(2) Gellman, S. H. *Acc. Chem. Res.* **1998**, *31*, 173.
(3) Schmuck, C. *Angew. Chem., Int. Ed.* **2003**, *42*, 2448.
(4) Okamoto, H.; Nakanishi, T.; Nagai, Y.; Kasahara, M.; Takeda, K. *J. Am. Chem. Soc.* **2003**, *125*, 2756.
(5) Fernandez-Lopez, S.; Kim, H. S.; Choi, E. C.; Delgado, M.; Granja, J. R.; Khasanov, A.; Kraehenbuehl, K.; Long, G.; Weinberger, D. A.; Wilcoxen, K. M.; Ghadiri, M. R. *Nature* **2001**, *412*, 452.
(6) Zhu, A.; Mio, M. J.; Moore, J. S.; Drickamer, H. G. *J. Phys. Chem. B* **2001**, *105*, 12374.
(7) Prince, R. B.; Barnes, S. A.; Moore, J. S. *J. Am. Chem. Soc.* **2000**, *122*, 2758.
(8) Nelson, J. C.; Saven, J. G.; Moore, J. S.; Wolynes, P. G. *Science* **1997**, *277*, 1793.
(9) Gin, M. S.; Moore, J. S. *Org. Lett.* **2000**, *2*, 135.
(10) Gin, M. S.; Yokozawa, T.; Prince, R. B.; Moore, J. S. *J. Am. Chem. Soc.* **1999**, *121*, 2643.
(11) Prince, R. B.; Saven, J. G.; Wolynes, P. G.; Moore, J. S. *J. Am. Chem. Soc.* **1999**, *121*, 3114.
(12) Brunsveld, L.; Meijer, E. W.; Prince, R. B.; Moore, J. S. *J. Am. Chem. Soc.* **2001**, *123*, 7978.
(13) Hill, D. J.; Moore, J. S. *Proc. Natl. Acad. Sci. U.S.A.* **2002**, *99*, 5053.
(14) Prince, R. B.; Okada, T.; Moore, J. S. *Angew. Chem., Int. Ed.* **1999**, *38*, 233.
(15) Tanatani, A.; Hughes, T. S.; Moore, J. S. *Angew. Chem., Int. Ed.* **2001**, *41*, 325.
(16) Tanatani, A.; Mio, M. J.; Moore, J. S. *J. Am. Chem. Soc.* **2001**, *123*, 1792.
(17) Elmer, S.; Pande, V. S. *J. Phys. Chem. B* **2001**, *105*, 482.
(18) Yang, W. Y.; Prince, R. B.; Sabelko, J.; Moore, J. S.; Gruebele, M. *J. Am. Chem. Soc.* **2000**, *122*, 3248.
(19) Sen, S. *J. Phys. Chem. B* **2002**, *106*, 11343.
(20) Cornell, W. D.; Cieplak, P.; Bayly, C. I.; Kollman, P. A. *J. Am. Chem. Soc.* **1993**, *115*, 9620.
(21) Bayly, C. I.; Cieplak, P.; Cornell, W. D.; Kollman, P. A. *J. Phys. Chem.* **1993**, *97*, 10269.
(22) Frisch, M. J.; Trucks, G. W.; Schlegel, H. B.; Scuseria, G. E.; Robb, M. A.; Cheeseman, J. R.; Zakrzewski, V. G.; Montgomery, J. A., Jr.; Stratmann, R. E.; Burant, J. C.; Dapprich, S.; Millam, J. M.; Daniels, A. D.; Kudin, K. N.; Strain, M. C.; Farkas, O.; Tomasi, J.; Barone, V.; Cossi, M.; Cammi, R.; Mennucci, B.; Pomelli, C.; Adamo, C.; Clifford, S.; Ochterski, J.; Petersson, G. A.; Ayala, P. Y.; Cui, Q.; Morokuma, K.; Malick, D. K.; Rabuck, A. D.; Raghavachari, K.; Foresman, J. B.; Cioslowski, J.; Ortiz, J. V.; Baboul, A. G.; Stefanov, B. B.; Liu, G.; Liashenko, A.; Piskorz, P.; Komaromi, I.; Gomperts, R.; Martin, R. L.; Fox, D. J.; Keith, T.; Al-Laham, M. A.; Peng, C. Y.; Nanayakkara, A.; Gonzalez, C.; Challacombe, M.; Gill, P. M. W.; Johnson, B.; Chen, W.; Wong, M. W.; Andres, J. L.; Gonzalez, C.; Head-Gordon, M.; Replogle, E. S.; Pople, J. A. *Gaussian 98*, revision A.7; Gaussian, Inc.: Pittsburgh, PA, 1998.
(23) Okuyama, K.; Hasegawa, T.; Ito, M.; Mikami, N. *J. Phys. Chem.* **1984**, *88*, 1711.
(24) Saebo, S.; Almlof, J.; Boggs, J. E.; Stark, J. G. *J. Mol. Struct.-THEOCHEM* **1989**, *200*, 361.
(25) MacKerell, A. D.; Bashford, D.; Bellott, M.; Dunbrack, R. L.; Evanseck, J. D.; Field, M. J.; Fischer, S.; Gao, J.; Guo, H.; Ha, S.; Joseph-McCarthy, D.; Kuchnir, L.; Kuczera, K.; Lau, F. T. K.; Mattos, C.; Michnick, S.; Ngo, T.; Nguyen, D. T.; Prodhom, B.; Reiher, W. E.; Roux, B.; Schlenkrich, M.; Smith, J. C.; Stote, R.; Straub, J.; Watanabe, M.; Wiorkiewicz-Kuczera, J.; Yin, D.; Karplus, M. *J. Phys. Chem. B* **1998**, *102*, 3586.
(26) Mohamadi, F.; Richards, N. G. J.; Guida, W. C.; Liskamp, R.; Lipton, M.; Caufield, C.; Chang, G.; Hendrickson, T.; Still, W. C. *J. Comput. Chem.* **1990**, *11*, 440.
(27) Grubmuller, H. *SOLVATE*, 1.2 ed.; Theoretical Biophysics Group, Institute for Medical Optics, Ludwig-Maximilians University: Munich, 1996.
(28) Humphrey, W.; Dalke, A.; Schulten, K. *J. Mol. Graphics* **1996**, *14*, 33.
(29) Jorgensen, W. L.; Chandrasekhar, J.; Madura, J. D. *J. Chem. Phys.* **1983**, *79*, 926.
(30) Kale, L.; Skeel, R.; Bhandarkar, M.; Brunner, R.; Gursoy, A.; Krawetz, N.; Phillips, J.; Shinozaki, A.; Varadarajan, K.; Schulten, K. *J. Comput. Phys.* **1999**, *151*, 283.
(31) Mackerell, A. D.; Wiorkiewiczkuczera, J.; Karplus, M. *J. Am. Chem. Soc.* **1995**, *117*, 11946.
(32) Feller, S. E.; Zhang, Y. H.; Pastor, R. W.; Brooks, B. R. *J. Chem. Phys.* **1995**, *103*, 4613.
(33) Martyna, G. J.; Tobias, D. J.; Klein, M. L. *J. Chem. Phys.* **1994**, *101*, 4177.
(34) Darden, T.; York, D.; Pedersen, L. *J. Chem. Phys.* **1993**, *98*, 10089.
(35) Karatas, T. 2000, unpublished.
(36) Stepanian, S. G.; Reva, I. D.; Radchenko, E. D.; Sheina, G. G. *Vib. Spectrosc.* **1995**, *11*, 123.
(37) Nelson, M. R.; Borkman, R. F. *J. Mol. Struct.-THEOCHEM* **1998**, *432*, 247.
(38) Pilkington, M.; Wallis, J. D.; Smith, G. T.; Howard, J. A. K. *J. Chem. Soc.-Perkin Trans. 2* **1996**, 1849.
(39) Chipot, C.; Jaffe, R.; Maigret, B.; Pearlman, D. A.; Kollman, P. A. *J. Am. Chem. Soc.* **1996**, *118*, 11217.
(40) Hunter, C. A.; Lawson, K. R.; Perkins, J.; Urch, C. J. *J. Chem. Soc., Perkin Trans. 2* **2001**, 651.
(41) Hunter, C. A.; Lu, X. J. *J. Mol. Biol.* **1997**, *265*, 603.
(42) Blatchly, R. A.; Tew, G. N. *J. Org. Chem.* **2003**, *68*, 8780.
(43) Kabsch, W. *Acta Crystallogr.* **1978**, *A34*, 827.
(44) Hunter, C. A.; Sanders, J. K. M. *J. Am. Chem. Soc.* **1990**, *112*, 5525.
(45) Hummer, G.; Rasaiah, J. C.; Noworyta, J. P. *Nature* **2001**, *414*, 188.
(46) Waghe, A.; Rasaiah, J. C.; Hummer, G. *J. Chem. Phys.* **2002**, *117*, 10789.
(47) Beckstein, O.; Biggin, P. C.; Sansom, M. S. P. *J. Phys. Chem. B* **2001**, *105*, 12902.
(48) Beckstein, O.; Biggin, P. C.; Bond, P.; Bright, J. N.; Domene, C.; Grottesi, A.; Holyoake, J.; Sansom, M. S. P. *FEBS Lett.* **2003**, *555*, 85.
(49) Stone, M. T.; Moore, J. S. *Org. Lett.* **2004**, *6*, 469.
(50) Jones, T. V.; Blatchly, R. A.; Tew, G. N. *Org. Lett.* **2003**, *5*, 3297.
(51) Heemstra, J. M.; Moore, J. S. *J. Am. Chem. Soc.* **2004**, *126*, 1648.
(52) Goldsmith, J. O.; Kuo, L. C. *J. Biol. Chem.* **1993**, *268*, 18481.
(53) DeLano, W. L. PyMOL Molecular Graphics System; San Carlos, CA, 2002.